Nanoscopy of Surface-Induced van der Waals-Zeeman Transitions

M. Hamamda[a], J. Grucker[a], G. Dutier[a], F. Perales[a], V. Bocvarski[b], J. Baudon[a] and M. Ducloy[a]

[a] *Laboratoire de Physique des Lasers, Université Paris 13, Av. J.B. Clément, 93430-Villetaneuse, France*
[b] *Institute of Physics-Belgrade, Pregrevica , PO Box , 11xxx-Zemun-Belgrade, Serbia*

Abstract. van der Waals transitions among magnetic sub-levels of a metastable rare gas atom passing near a surface immersed in a magnetic field, are described. Related transition amplitudes are calculated using both the sudden and the Landau-Zener approximations. Experimental data for Ne*($^3P_2$) atoms traversing a copper grating are presented. For a pair of surfaces (*e.g.* the opposite edges of a slit) and a sufficiently large coherence width, Fresnel's biprism interference fringes are obtained. From this interference pattern, detailed information about the transition amplitude at a sub-nanometric scale can be derived. The effect of gravity on this pattern is examined.

Keywords: surface, anisotropic van der Waals interaction, metastable atoms, coherent atom optics, interferometry, diffraction

PACS: 03.75.Be Matter waves; Atom and neutron optics
37.25.+k Atom interferometry techniques
34.-35.+a Interactions of atoms and molecules with surfaces

1. INTRODUCTION

Till relatively recent years, it was commonly admitted that the interaction at moderate distance (1-100 nm) between an atom and a planar or quasi-planar solid surface, was a simple scalar attractive potential of the (non retarded) van der Waals (vdW) type in d^{-3}, where d is the atom-surface distance. Actually this statement is based upon assumptions which are not fulfilled in many real situations. Firstly the solid is assumed to behave passively, which is only true for a perfect conductor. Indeed for a real conductor or a dielectric body the frequency dependence of the permittivity, $\varepsilon(\omega)$, (and occasionally that of the magnetic permeability μ) is involved. This is of a special importance when an atom-solid resonance occurs, giving rise in some cases to a repulsive rather than an attractive interaction [1]. Secondly, for non-planar surfaces the curvature radius of which is sufficiently small (a few nm), the distance dependence, while remaining calculable – at least in the case of a perfect metal – by use of the electrostatic-image method, departs from d^{-3}. Last but not least, for atoms not in a S- state, such as rare gas metastable atoms heavier than helium, a quadrupolar term is added to the previous scalar contribution. This leads, for a perfect conductor, to the total interaction operator:

$$V_{vdW}(d) = -(64\,\pi\,\varepsilon_0\,d^{3})^{-1}\,[4\,\mathbf{D}^2/3 + (\mathbf{D}.\mathbf{n})^2 - \mathbf{D}^2/3] \qquad (1)$$

where **D** is the atomic dipole operator and **n** the normal to the surface. The quadrupolar term, proportional to $(\mathbf{D}.\mathbf{n})^2 - \mathbf{D}^2/3$, breaks the atomic- (or molecular-) state symmetry and is able to induce a wide variety of transitions. Almost all types of such transitions have been experimentally observed so far: fine structure transitions ($^3P_0 \leftrightarrow {}^3P_2$) in Ar* and Kr* [2], vibrational transitions ($v + 1 \leftrightarrow v$) in metastable nitrogen molecules $N_2^*(A^1\Sigma_u^+)$ [3]. When an external static magnetic field **B** is applied, a Zeeman contribution ($g\,\mu_B\,m\,B$) is added to the interaction (1), where g is the Landé factor, μ_B is the Bohr magneton and m the magnetic number. The Zeeman term is diagonal only in the Zeeman-state basis set, referred to the quantization axis **B**. On another hand the atom-solid

CP1058, *Spectral Line Shapes, Vol. 15, 19th International Conference*
edited by M. A. Gigosos and M. Á. González

interaction refers to the normal **n** to the surface. In such a situation where two different quantization axes are involved, transitions among Zeeman states – so-called "van der Waals-Zeeman (vdW-Z) transitions"– are expected. These transitions, which have been already observed in Ne*($^3P_2$) [4] and later in Ar*($^3P_2$), will be the central subject of this paper. In part 2, the principle and two approximations used in the calculation of the transition amplitude are briefly presented and the main characteristics of this amplitude are described. Then an experimental evidence for vdW-Z transitions is given. In part 3 an atomic biprism interferometer based upon vdW-Z transitions occurring at the two borders of a slit is described. The influence of gravity on this device is also examined.

2. VAN DER WAALS – ZEEMAN TRANSITIONS

Calculation of the Transition Amplitudes

Within the initial velocity range considered here ($v_0 \geq 5$ m/s) and owing to the atomic masses under consideration (M ≥ 20 a.m.u), a semi-classical description of the atomic external motion is fully justified. Moreover, because of the smallness of the deflection angles caused by the interaction, a quasi-straight line trajectory, parallel to $\hat{z}$ axis, along which the atom velocity is practically a constant (v_0), can be assumed. This trajectory passes in the vicinity of a solid surface modelled by a cylinder whose radius *a* is of the order of 1 μm (the exact value is of no importance provided it is large enough). At the distance of minimum approach ρ, the normal **n** is perpendicular to $\hat{z}$ ($\hat{x}$ axis). As it will be seen further, the transition probability A(ρ) rapidly drops down to zero as soon as ρ exceeds $\rho_M \approx 3$ nm << *a*. As a consequence, as the atom-surface distance at abscissa z, $d(\rho,z) = [z^2 + (a + \rho)^2]^{1/2} - a$, is larger than ρ, the interaction with the surface is restricted to a range in z much smaller than *a*. In other words the normal **n** rotates by a negligible angle during the passage of the atom through the region of interaction. Consequently the angle $\chi = (\mathbf{n},\mathbf{B}) \approx (\hat{x},\mathbf{B})$ can be considered as constant. Using the Wigner-Eckart theorem, one can express the vdW potential with the atomic angular momentum **J** instead of **D**. Finally the total potential experienced by the atom is:

$$V(\rho,z) \approx g\,\mu_B\,\mathbf{J}.\mathbf{B} - d(\rho,z)^{-3}\{C_3 + (\eta/16)\,[(\mathbf{J}.\mathbf{n})^2 - \mathbf{J}^2/3]\} \qquad (2)$$

where C_3 and η are real constants characterising respectively the scalar and the quadrupolar parts of the vdW potential (in the case of Ar*, in atomic unit, $C_3 = 2.23 \pm 0.03$, $\eta = -0.20 \pm 0.08$).

In the *sudden approximation*, valid at large enough velocity (typically larger than 50 m/s), the surface-interaction time is supposed to be very small compared to the Larmor period in the magnetic field **B**. Under such conditions, the inelastic amplitude for the transition m → m', with m' < m, is given by [5]:

$$A_{m,m'}(\rho,v_0) = \langle m | \exp[-i\,\alpha(\rho,v_0)\,J_x^2] | m' \rangle \qquad (3)$$

where

$$\alpha(\rho,v_0) = 3\pi\,\eta\,(128\,\hbar\,v_0)^{-1}\,(2a/\rho^5)^{1/2} \qquad (4)$$

Completely analytical expressions of the $A_{m,m'}$-s can then be derived from (3), knowing the matrix elements $\langle m | J_x^2 | m' \rangle$. For a non-polarized incident beam, the transition probability for a given value of $\Delta m = m' - m < 0$, is given by: $P_{\Delta m} = \frac{1}{2J+1}\sum_m \left|A_{m,m-|\Delta m|}\right|^2$. As an example, the behaviour of $A_{0,-1}$ as a function of ρ is shown in fig.1, for Ne* atoms at velocity $v_0 = 780$ m/s.

In the *quasi-adiabatic approximation*, the eigenvalues of (2) are determined for each z value, at a given value of ρ. It worth to be noted that, for our purpose, the scalar term (-

C_3/d^3) can be ignored since it results into a shift common to all eigenvalues. Obviously if one assumes that, when z varies from $-\infty$ to $+\infty$, the system adiabatically follows one of these eigenvalues (defined by the initial m value), then no transition occurs. However this evolution cannot be purely adiabatic because the potential curves exhibit either crossings, for $\chi = 0$, or avoided crossings for $\chi \neq 0$. This is readily seen from the very simple expression of the dimensionless "reduced" potential V_r (*i.e.* the non scalar potential normalized by the Zeeman factor $g\,\mu_B\,B$), as a function of the new variable:

$$\beta = -\,\eta\,(16\,g\,\mu_B\,B)^{-1}\,d(\rho,z)^{-3}\ , \qquad (5)$$

namely:
$$V_r(\beta) = J_{z'} + \beta\,[J_x^{\,2} - \mathbf{J}^2/3]\ , \qquad (6)$$

the z'-axis being collinear to **B**. For J = 2 and $\theta = 0$, five straight lines are obtained, crossing at four points (β = 1/3, 1/2, 1, 1).

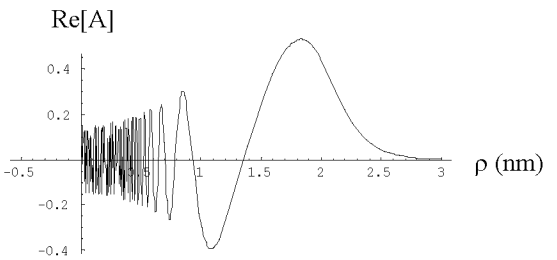

FIGURE 1. Real part of the vdW-Z transition amplitude $A(\rho)$ for Ne* atoms (velocity v_0 = 780 m/s), calculated in the sudden approximation, as a function of the distance of closest approach ρ (in nm); B= 289 G, angle $\chi = (\mathbf{n},\mathbf{B}) = 12°$ (see text).

For $\chi \neq 0$, these crossings become avoided (at small angles, the separations in V_r are respectively χ, $5\chi^2/2$, $\sqrt{3/2}\,\chi$, $3\chi^2/4$), but they remain in most cases well isolated from each other. This justifies the use of the well known Landau-Zener formula [6] to evaluate the amplitudes emerging from each crossing. Then, starting from a given entrance channel (m) and taking in account the phase shifts developed along all the possible paths connecting m to a specific output channel (m'), one is able to calculate the amplitude $A_{mm'}(\rho)$. At intermediate velocity (around 50 m/s), the inelastic amplitude is close to that given by the sudden approximation. The interesting point here is that the quasi-adiabatic approximation remains valid at lower velocities. In particular it is seen that, for Ar* atoms, the intensity $|A|^2$ increases by a factor of about 40 when v_0 decreases from 560 m/s down to 5.6 m/s. It is then a great advantage to slow down the atoms. This has been done for Ar*($^3P_2$) atoms, using a Zeeman slower operating with a laser frequency maintained in resonance with the $^3P_2$-$^3D_3$ atomic closed transition (λ = 811.5 nm) by means of a special longitudinal magnetic-field profile.

Two main features appear in $A(\rho)$: (i) a very limited range (ρ_M) in ρ, within which A is not zero, (ii) an oscillatory behaviour. Owing to typical distances used in a standard experiment, the diffraction of the inelastic wave packet produced by vdW-Z transitions near the surface takes place in the Fraunhofer regime. This means that the amplitude $B(\theta)$ diffracted at angle θ with respect to the incident direction $\hat{z}$ is simply the Fourier transform of $A(\rho)$. Therefore the two main features in $A(\rho)$ appear in $B(\theta)$ as: (i) a finite angular width $\Delta\theta \sim \lambda/\rho_M$, (ii) a shift γ with respect to the $\hat{z}$ direction. Whilst $B(\theta)$ is directly calculable, one

can more clearly exhibit these two features by using, for $A(\rho)$, a very simple model, namely: $A_0(\rho) = C(\rho) \exp(i\Omega\rho)$, where C is a square-shaped function ($C = 1$ for $\rho \leq \rho_M$, $C = 0$ elsewhere); Ω is an averaged spatial frequency. In this case, one readily gets:

$$B_0(\theta) = FT[A_0(\rho)] = 2\,\rho_M \exp[i(k\theta - \Omega)\,\rho_M]\ \mathrm{Sinc}[(k\theta - \Omega)\,\rho_M] \qquad (7)$$

where $\mathrm{Sinc}(x) = \sin(x)/x$. This expression clearly exibits both the angular shift $\gamma = \Omega/k$ and the angular width of the diffracted peak, $\Delta\theta = \lambda / (2\rho_M)$. The angle γ can be directly derived from momentum-energy conservation rules. Indeed the process, assumed to be exo-energetic by an amount ΔE, generates a momentum change Δp along **n**. Then γ being a small angle,

$$\gamma \approx \Delta p / p_0 = (\Delta E / E_0)^{1/2} \qquad (8)$$

, where p_0 is the initial momentum (parallel to $\hat{z}$) and E_0 the initial kinetic energy. For a given negative value of Δm, one gets:

$$\gamma \approx (g\mu_B B|\Delta m| / E_0)^{1/2} \qquad (9)$$

Hence the mean spatial frequency

$$\Omega = k\gamma = (2g\mu_B B|\Delta m|\, M)^{1/2} / \hbar \qquad (10)$$

is independent of the initial velocity.

Experimental Evidence of vdW-Z Transitions

Experiments have been carried out with a beam of "fast" atoms, $Ne^*(^3P_2)$ ($v_0 = 780$ m/s) [4, 5] and $Ar^*(^3P_2)$ ($v_0 = 560$ m/s) traversing an inclined copper grating. The applied magnetic field B ranges from 150 to 600 Gauss. Figure 2a shows the angular distribution observed with Ne* atoms, B = 289 Gauss, $\chi = 12°$. Actually this distribution is the difference of signals obtained with and without B (the background line is the difference of two signals obtained with B = 0). A series of peaks are seen. They are related to vdW-Z transitions with $\Delta m = -1, -2, -3$ (vertical arrows show γ values derived from (9)). These peaks are much wider than the incident beam profile (blue line) because of the diffractive spreading $\Delta\theta$ (the dotted line is a simulation of this effect). This experiment has been repeated at different values of B. As shown by eq. (9), in a diagram (γ, $B^{1/2}$), each Δm value corresponds to a straight line, as it is seen in figure 2b (without any adjustable parameter). To conclude, the system surface + **B** operates as an adjustable (*via* B) atomic beam splitter, potentially usable in atom interferometry. The next paragraph will describe such an application.

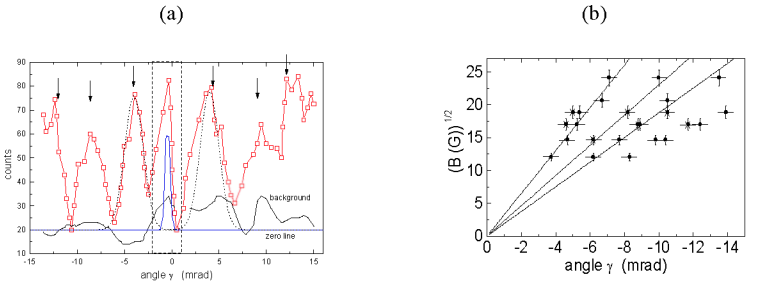

FIGURE 2. (a) Inelastic diffraction pattern; vdW-Z transitions with $\Delta m = -1, -2, -3$ are indicated by vertical arrows; blue line: incident profile; full line: background; dotted line: diffracted peak calculated for $\Delta m = -1$. (b) Experimental peak locations in the diagram (γ, $B^{1/2}$); straight lines are those given by eq.(9) (see text).

3. ATOMIC FRESNEL BIPRISM, SCHLIEREN NANOSCOPY

Principle. Expected interference pattern

Let us consider two opposite surfaces, *e.g.* the two edges of a slit, symmetric with respect to the z-axis at distances ± w/2 along the x-axis, with w >> ρ_M. These surfaces are immersed in an homogeneous magnetic field **B** making angles χ and $\pi-\chi$ (equivalent as concerns the transition amplitudes) with opposite normal vectors ± **n**. We consider here a beam of slow atoms (Ar* ($^3P_2$) at v_0 = 56 m/s), whose transverse coherence diameter is larger than w. Under such conditions, for a given value of Δm (< 0), two narrow and mutually coherent wave packets are generated. As seen before they are deflected by opposite angles ± γ while they are strongly spread by diffraction (angular width $\Delta\theta$). Beyond a certain distance from the slit, namely $z \geq w/(\gamma + \Delta\theta/2)$, they overlap and produce, along the x direction, non-localized interference fringes. These fringes are similar to those produced by a Fresnel biprism [7].

The diffraction regime depends on the Fresnel number, here $F = w\,(\lambda z)^{-1/2}$. For Ar* atoms at a velocity v_0 = 56 m/s, the wavelength is λ = 0.18 nm. Hence for w = 1μm, the Fraunhofer regime is reached as soon as z >> 5.5 mm, a condition we shall assumed to be fulfilled in the following. Therefore the diffraction amplitude U(θ) produced by the pair of surfaces is simply the Fourier transform of the double transition amplitude: A(w/2 + x) + A(w/2 – x). As w/2 >> ρ_M, these two contributions do not overlap which immediately gives:

$$U(\theta) = \exp(-ikw\theta/2)\, B(\theta) + \exp(+ikw\theta/2)\, B(-\theta) \qquad (11)$$

The corresponding intensity is:

$$I(\theta) = \left| B(\theta) \right|^2 + \left| B(-\theta) \right|^2 + 2 \left| B(\theta)\, B(-\theta) \right| \cos\left[kw\,\theta - \varphi(\theta) + \varphi(-\theta)\right] \qquad (12)$$

where φ is the argument of B. Fringes correspond to the cosine term. For $\theta \neq 0$, the fringe splitting is modified by the phase shift between B(θ) and B(-θ). Similarly the fact that $B(\theta) \neq B(-\theta)$ leads to a limitation of the contrast: $\Gamma = (I_{max} - I_{min})/(I_{max} + I_{min}) = 2\left|B(\theta)\, B(-\theta)\right| / \left[\left|B(\theta)\right|^2 + \left|B(-\theta)\right|^2\right]$. Actually Γ is more severely limited by the velocity dispersion $\delta v_0/v_0$ of the incident beam since the number of visible fringes is limited to $v_0/\delta v_0$, i.e. to about 100. Other factors are expected to limit the fringe visibility: (i) the inclination of the interaction-zone line by some (small) angle with respect to the x axis has a quite negligible effect; (ii) the roughness of the slit borders adds a random contribution (ξ) to the width w; this also leads to a limitation of the visible fringe number given by $w/(\langle\xi^2\rangle)^{1/2}$, where <> is a statistical average; owing to realisable mechanical accuracy, this number (~10^3) is much larger than that imposed by the velocity dispersion and the roughness effect can be neglected. A third effect, which depends on the orientation of x with respect to the vertical direction, is also worth to be examined, namely the effect of gravity.

Effect of gravity on the interference pattern

The effect of gravity on Young-slit interference fringes has been investigated in the past by Shimizu *et al.* [8]. It has been also considered in the case of a three-grating atomic interferometer [9]. Here the effect is expected to be particularly important when the $\hat{x}$ direction is vertical, whilst it is negligible for $\hat{x}$ horizontal. Hence we shall restrict the discussion to the former case. A linear (parallel to $\hat{y}$) and monochromatic (velocity v_0) atom source Σ crosses the z-axis at the origin (see figure 3). In a semi-classical (eikonal) description of the external motion, the rays related to the atomic wave are the classical

trajectories. Only z and x coordinates need to be considered. It is easy to verify that two such trajectories ("lower" and "upper" trajectories) join the source Σ to a given point Q (of coordinates Z, X), provided that:

$$X \leq 1 / (4\,a^2) - a^2\,Z^2 \qquad (13)$$

where $a^2 = g / (2v_0^2)$, g being the gravity constant. For $v_0 = 56$ m/s and $g = 9.81$ m/s^2, one has: $a^2 = 0.00156$ m^{-1}. When (13) is not fulfilled, no trajectory exists. This behaviour of the rays reflects that of the atomic wave: close to Σ it is practically a diverging cylindrical wave. Then it "falls" and overlaps with itself, giving two contributions at any point Q whose coordinates satisfy eq.(13), otherwise the wave cannot reach the point. The source being assumed isotropic, the amplitudes of these two coherent contributions are proportional to the angular apertures dφ, dφ' within which lower and upper trajectories have to start in order to reach a given interval of width dX around X. Owing to the values of v_0 and the distances considered here, it is easy to verify that the upper-wave contribution is totally negligible. It will be ignored in the following calculation.

For our purpose, the key quantity to be evaluated is the phase developed along the ray joining Σ to Q. According to the eikonal approximation, this phase is given by:

$$\phi(Q) = \int_{\Sigma}^{Q} \mathbf{K}.d\mathbf{s} \qquad (14)$$

where $\mathbf{K} = M\mathbf{v} / \hbar$ is the local wave vector, M being the atom mass and **v** the local velocity. As the integral is evaluated along the ray, **K** and the elementary displacement d**s** are collinear. Then:

$$\phi(Q) = \frac{M}{\hbar} \int_0^{\tau} v(t)^2\, dt \qquad (15)$$

where τ is the arrival time at point Q.

In a general case, let us call β the angle between the z-axis and the velocity vector at the starting point. For given values of Z and X, with the condition $X \leq (4a^2)^{-1} - a^2Z^2$, one has:

$$T(Z,X) = \tan\beta = (2a^2Z)^{-1}\,[1 - (1 - 4a^2\,(X + a^2Z^2))^{1/2}] \qquad (16)$$

Then, for instance, the phase developed from Σ(0, 0) to S(L, w/2) has the analytic expression (equivalent to that given in [9]):

$$\phi = \frac{Mv_0}{\hbar}\,(1 + T_\Sigma^2)^{1/2}\,[L - 2a^2T_\Sigma L^2 + 4a^4(1 + T_\Sigma^2)L^3] \qquad (17)$$

where $T_\Sigma = T(L, w/2)$. The phase φ' developed from Σ to S' has the same expression, T_Σ being replaced by $T_\Sigma' = T(L, -w/2)$. As a consequence a phase shift appears between the two secondary sources S, S'. Then each of these sources is assumed to re-emit an isotropic wave, in phase with the wave it receives. Similar expressions are readily obtained for the phases

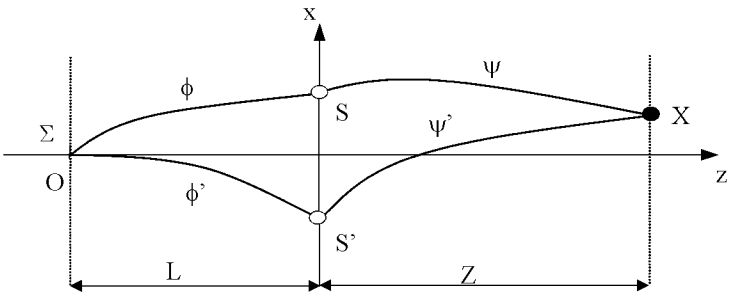

FIGURE 3. Classical trajectories used in the semi-classical calculation of the phases ϕ, ϕ' developed from the source Σ to Young slits S, S', and those, ψ, ψ', developed from S, S' to the observation point P.

ψ, ψ' developed from S or S' to the observation point P, by changing L into Z and $\pm$ w/2 into X $\mp$ w/2. Finally the *geometrical* phase shift (here one ignores the additional term ($\varphi(\theta) - \varphi(-\theta)$) present in eq.(12)) governing the interference is $\Delta = \phi + \psi - \phi' - \psi'$.
By making g = 0, *i.e.* $a^2 = 0$, one recovers the "ordinary" phase shift (Δ_0) that appeared in (12). Indeed, in such a case, the different phases become ϕ_0, ϕ_0' with $\phi_0 - \phi_0' = 0$ and

$$\psi_0^{(')} = \frac{Mv_0}{\hbar}[(X \mp w/2)^2 + Z^2]^{1/2} \qquad (18)$$

which gives, for $|X|$ and w small compared to Z,

$$\Delta_0 = \psi_0 - \psi_0' \approx - k\, w\, X/Z = - k\, w\, \theta \qquad (19)$$

The main effect of g is a vertical shift of the central fringe. However, from an experimental point of view, gravity cannot be turned on and off so easily. One possibility is to rotate the slit SS' by 90° around z, making horizontal the x-axis. In spite of the difficulty to guarantee the strict invariance of other parameters during this operation, a qualitative characterisation of the effect is expected. Another possibility is to compensate gravity by an appropriate vertical magnetic gradient **G**. The difficulty is that the secondary sources S, S' are generated by a vdW-Z transition, so that the magnetic number m, and correlatively the effect of the gradient, is different for z < L and z > L. Nevertheless, in the special case of a transition from m = +1 to m' = 0, the effect of gravity can be compensated for z ≤ L, while it is not for L < z ≤ L+Z. Consequently this will only affect the phase shift $\phi - \phi'$ induced by gravity between the two secondary sources. It is worth to note that the required gradient is easy to realize. It is simply given by: $G = Mg/(g_L\mu_B)$ (here the Landé factor is noted g_L to be distinct from the gravity constant g). For Ar* atoms this gives G ≈ 3.54 Gauss/cm. In fact this gradient can be scanned from zero up to this value, and even beyond, giving a way to vary gravity along the first half part of the experiment. An example of the effect of the magnetic gradient is shown in figure 4, for Ar* atoms at velocity v_0 = 5.6 m/s traversing a slit of width w = 1 μm.

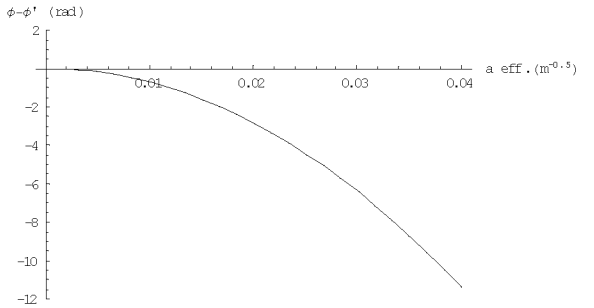

FIGURE 4. Combined effect of gravity and vertical magnetic gradient G on the phase shift ($\phi - \phi'$) between the two secondary sources (see text). The variable a_{eff} (in $m^{-1/2}$) is defined by $a_{eff}^2 = (g - g_L\mu_B\, G/M) / (2v_0^2)$. For G = 0, one has $a_{eff} = a = 0.0395\ m^{-1/2}$.

The authors are members of the *Institut Francilien de Recherche sur les Atomes Froids* (IFRAF).

REFERENCES

1. H. Failache, S. Saltiel, M. Fichet, D. Bloch and M. Ducloy, Phys. Rev. Lett., **83**, 5467 (1999)
2. M. Boustimi, B. Viaris de Lesegno, J. Baudon, J. Robert and M. Ducloy, Phys. Rev. Lett. **86**, 2766, 2001
3. M. Boustimi, J. Baudon, F. Pirani, M. Ducloy, J. Reinhardt, F. Perales, C. Mainos, V. Bocvarski and J. Robert, Europhys. Lett., **56**(5), pp.644-650 (2001) ; J.-C. Karam, J. Grucker, M. Boustimi, G. Vassilev, J. Reinhardt, C. Mainos, V. Bocvarski, J. Robert, J. Baudon, F. Perales
J. Phys. B : At. Mol. Opt. Phys. **39**, 1837 (2006)
4. J.-C. Karam, J. Grucker, M. Boustimi, F. Perales, V. Bocvarski, J. Baudon, G. Vassilev, J. Robert, M. Ducloy Europhys. Lett., **74**, 36 (2006)
5. J.-C. Karam, PhD Thesis, University Paris 13 (2005)
6. J. Grucker, PhD Thesis, University Paris 13 (2007)
7. J. Grucker, J. Baudon, F. Perales, G. Dutier, V. Bocvarski, J.-C. Karam, G. Vassilev, M. Ducloy, The European Physical Journal D, **47**, 427 (2008)
8. F. Shimizu, K. Shimizu and H. Takuma, Phys. Rev. **A 46**, R17 (1992)
9. J.-C. Karam, J. Baudon, F. Perales, M. Ducloy and J. Robert, Proc. 38th *Rencontres de Moriond*, Les Arcs, France (2003)